

# Influence of Poly(arylether sulfone) Molecular Weight Distribution on Measures of Global Thermal Stability

LINDA J. BROADBELT,<sup>1,\*</sup> MICHAEL T. KLEIN,<sup>1,†</sup> BARRY D. DEAN,<sup>2</sup> and STEPHEN M. ANDREWS<sup>2</sup>

<sup>1</sup>Center for Catalytic Science and Technology, Department of Chemical Engineering, University of Delaware, Newark, Delaware 19716; <sup>2</sup>Amoco Performance Products, Inc., Alpharetta, Georgia 30202

## SYNOPSIS

The dependence of the thermal stability of high-performance poly(arylether sulfones) (PAES) on the initial molecular weight distribution and backbone structure was assessed experimentally and through computer simulation. Reaction of PAES polymers resulted in the formation of an insoluble gel fraction and significant changes in weight and number average molecular weights of the sol fraction. A PAES with alternating ether and sulfone linkages formed a larger fraction of gel at a given reaction time than a PAES with the hydroquinone moiety. For a given chemical composition, more rapid molecular weight changes and gel fraction formation were observed for the polymer with the higher value of the initial weight average molecular weight. The growth of molecular weight was also faster for the polymer with the broader initial distribution. The simultaneous increase in  $M_w$  and decrease in  $M_n$  suggested the occurrence of two types of overall reactions: scission and addition. Simulation of these reactions using Monte Carlo kinetics allowed estimation of the range of probability for bond scission,  $R$ , of  $0.5 < R < 0.8$  capable of accounting for the observed experimental behavior. The dependence of the simulated molecular weight changes on the initial molecular weight distribution agreed qualitatively with the experimental trends. © 1995 John Wiley & Sons, Inc.

## INTRODUCTION

Sulfone-containing polyarylethers generally include one or more aromatic rings linked together by ether and sulfone groups. One class of these polymers also contains isopropylidene linkages. They form a class of polymers that is tough, has a high softening temperature, and maintains desirable properties for extended periods of time.<sup>1,2</sup>

Neat poly(arylether sulfones) are softened by heating for processing. Rose<sup>2</sup> suggests that some of the challenges to this processing are engendered by the valuable properties of the polymers themselves. The same desirable high temperature softening point for end-use applications is also high enough that some thermal degradation can occur during front-

end processing. This can lead to gas evolution and viscosity increase, the latter presumably owing to the formation of a gel. Thus, many studies into poly(arylether sulfone) thermal stability have sought optimal conditions and formulations to minimize the deleterious effects of exposure to high temperature.

Previous investigations of poly(arylether sulfone) (PAES) thermal stability have focused on the link between the identity and proportion of various backbone linkages and the reactivity of the polymer. Primarily, comparisons have been made between PAES polymers with and without the isopropylidene link. Hale and co-workers<sup>3</sup> examined the stability of the isopropylidene-containing PAES in argon, air, and vacuum at temperatures above 400°C. They proposed a series of bond scissions dictated by the relative strengths of the linkage bonds to account for the evolution of sulfur dioxide, methane, and other small decomposition products. Molecular weight growth via crosslinking was not proposed. Levantovskaya et al.<sup>4</sup> specifically considered the

\* Present address: Department of Chemical Engineering, Northwestern University, Evanston, IL 60208.

† To whom correspondence should be addressed.

hydrolytic and oxidative stability of isopropylidene-containing PAES. An observed increase in the intrinsic viscosity was accounted for by the dominance of "structurization" over degradation processes, but no mechanism was proposed.

Crossland and co-workers<sup>5</sup> compared the thermal stability of PAES polymers in air and an inert atmosphere using thermogravimetry. They accounted for all degradation products on the basis of chain scission and hydrogen abstraction reactions. Danilina et al.<sup>6</sup> reacted five different poly(arylether sulfones) in vacuum and measured the gel content as a function of heating time. The isopropylidene-containing polymer showed a 2-h induction period for gel formation, whereas the kinetics of gel formation for the sample composed solely of sulfone and ether linkages were rapid under the conditions studied. They proposed phenyl addition to backbone aromatic rings as the primary mechanism for gel formation. In both of these studies, no uniformity in the initial molecular weight distributions among the polymers of different chemical composition was maintained.

A more quantitative analysis was performed by Davis<sup>7</sup> who examined the degradation of the isopropylidene-containing PAES with and without removal of volatile products. Rate constants for scission and crosslinking were estimated by fitting the gel fraction data to the form of the Charlesby and Pinner equation.<sup>8</sup> The values  $k_s = 0.78 \times 10^{-3} \text{ h}^{-1}$  and  $k_x = 2.6 \times 10^{-3} \text{ h}^{-1}$  were insensitive to the presence of evolved reaction gases. Kuroda et al.<sup>9</sup> favored quantitative analysis of thermal degradation via measurement of the molecular weight changes of the sol fraction because of the smaller sample sizes required and the poor solubility of aromatic polymers. They predicted the ratio of scission to addition for a series of PAES polymers by correlating weight and number average molecular weight changes with random crosslinking and chain scission reactions. Quantitative disagreement with the values reported by Davis was explained by the difference in the time scales required for molecular weight changes and gel fraction measurements.

Clearly, ambiguity in the quantitative link between formulation molecular weight distribution and reactivity still exists. Reliable quantitative estimates of kinetic phenomena are not currently available. Previously reported values were dependent upon the experimental protocol used. Furthermore, little attention has been paid to determining the relationship between reactivity and physical properties for a PAES of a given chemical composition.

These needs motivated the current work aimed at examining the dependence of PAES thermal reactivity on the initial molecular weight distribution. The initial molecular weight distribution has both physical and chemical implications. A polymer with a high molecular weight tail in the initial distribution inherently possesses the precursor to a high molecular weight, insoluble gel fraction. Nakron et al.<sup>10</sup> reported that a PAES polymer with solely hydroxyl end groups was less thermally stable than one with methoxy end groups. This dependence on the chemical identity of the end groups suggests that the number of end groups also plays an important role in determining thermal stability. The number of end groups present and the initial molecular weight distribution are inexorably linked.

Two parameters of the distribution were varied in the present analysis: the value of the second moment, or the weight average molecular weight, and the breadth of the distribution as measured by the polydispersity. First, the initial weight average molecular weight was fixed while the breadth of the distribution was varied. Second, the initial weight average molecular weight was varied at a relatively constant value of polydispersity. A Monte Carlo kinetics simulation was developed for comparison with the experimental results to probe the reactivity/property relationships quantitatively.

## EXPERIMENTAL

Two representative poly(arylether sulfones) were pyrolyzed. Commercial samples of ICI polyether-sulfone (PES) possessing the repeat unit shown in

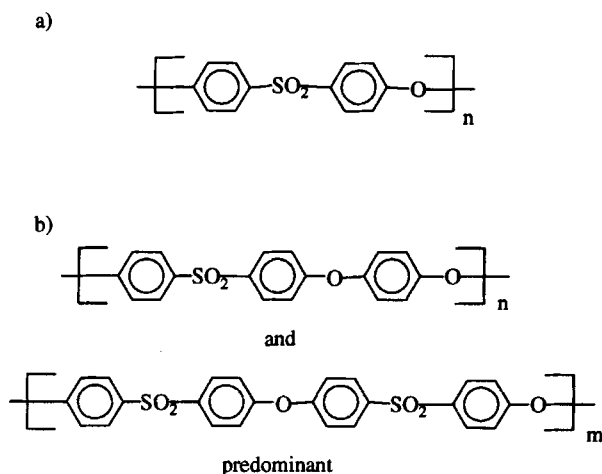


**Figure 1** Repeat units of poly(arylether sulfones). (a) PES, (b) PHS.

**Table I** Characterization of Initial PES and PHS Polymers in Terms of Number Average and Weight Average Molecular Weights

Polymer	Symbol	$M_w$	$M_n$	$M_w/M_n$
PES	PES <sub>b</sub>	50000	5000	10.0
PES	PES <sub>n</sub>	57401	23381	2.46
PHS	PHS <sub>n</sub>	132646	9278	14.3
PHS	PHS <sub>i</sub>	27970	3548	7.88

Figure 1(a) were representative examples of polymers with significantly different polydispersities at an essentially constant value of weight average molecular weight. Samples of a PAES possessing the hydroquinone moiety (PHS), with the repeat unit shown in Figure 1(b), had different initial weight average molecular weights but similar values of polydispersity. Characterization of the initial molecular weight distributions in terms of the first and second moments of the distribution, number average molecular weight ( $M_n$ ) and weight average molecular weight ( $M_w$ ), respectively, is presented in Table I. The polymers are hereafter referred to using the symbols in column 2 of Table I.

Neat pyrolysis reactions were carried out at 425°C in an inert argon atmosphere for batch reaction times typically ranging from 5 to 240 min. The reactors were 2-mL glass ampoules (Wheaton). Approximately 40 mg of polymer was placed in the glass ampoule, which was purged and flame sealed. This reactor was then placed in an isothermal fluidized sand bath for the predetermined reaction time. The time required to achieve the reaction temperature of 425°C was determined to be 2 min. After the duration of the reaction time, the reactor was removed and cooled at room temperature. The reactor was reweighed to check for leakage.

The reaction products were grouped into three different global fractions: gas fraction, gel fraction, and sol fraction.<sup>11</sup> The defining analytical procedures were as follows.

For gas analysis, the vial was opened in a sampling vessel of predetermined volume wherein the gases were allowed to equilibrate with mixing for 8 h. Gas aliquots of 1 mL were injected into a Perkin-Elmer Sigma 3b chromatograph equipped with a flame photometric detector, allowing quantification of sulfur-containing compounds.

The gel fraction was defined by a combined solubility/filtration protocol. After the gas analysis was completed, the polymer was extracted from the reaction vial with repeated washings of dichloromethane. This liquid sample was then passed through

1.0- and 0.45- $\mu$ m polytetrafluoroethylene filters in series, and the soluble fraction (sol fraction) was collected. The preweighed filter was then dried in a vacuum oven at 80°C for 24 h. Subsequent weighing provided the weight of the solid fraction. The gel fraction was calculated by dividing the weight of the solid fraction by the initial weight of the polymer.

The molecular weight distribution of the sol fraction was analyzed on a Hewlett Packard 1090M liquid chromatograph using gel permeation chromatography. A Hewlett Packard PL gel linear column was used in series with a Hewlett Packard 50 Å column. A refractive index detector was employed. The solvent was dichloromethane at a flow rate of 0.8 mL/min. Calibration was performed using narrow molecular weight distribution polystyrene standards from Scientific Polymer Products. The possibility that low-molecular-weight liquid products formed was checked by gas chromatography using an HP5890 gas chromatograph equipped with a flame ionization detector and an Ultra 2 5% crosslinked phenyl methyl silicone capillary column. Dibenzyl-ether was added as an external standard.

## EXPERIMENTAL RESULTS

### Gas Analysis

Sulfur dioxide ( $\text{SO}_2$ ) was the major gas product from reaction of both polymers. The time dependence of the quantitative yield from PES<sub>b</sub>, calculated as the mass of evolved  $\text{SO}_2$  divided by the mass of  $\text{SO}_2$  units in the polymer, is presented in Figure 2 as representative. The rate of  $\text{SO}_2$  evolution decreased monotonically with increasing reaction time. The quantity of other sulfur-containing gases was neg-

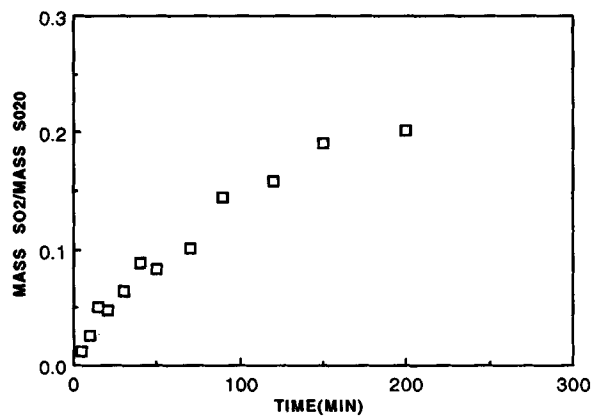


**Figure 2** Evolution of sulfur dioxide as the major volatile reaction product from PES pyrolysis at 425°C.

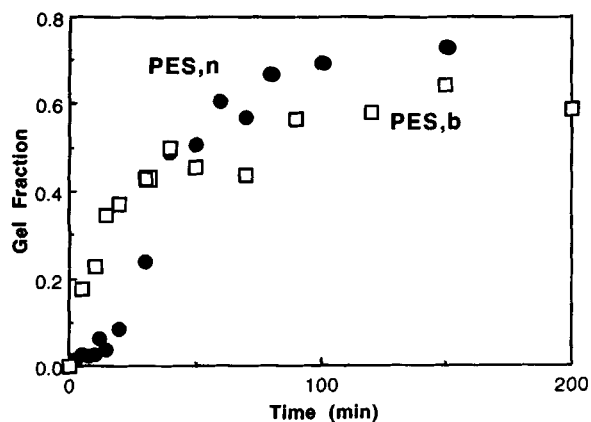


**Figure 3** Comparison of the temporal variations of gel formation for PES polymers with different initial molecular weight distributions (PES<sub>b</sub> = broad; PES<sub>n</sub> = narrow).

ligible. Moreover, quantitative GC analysis revealed that no liquid phase lower molecular weight products indicative of bond scission formed.

### Gel Fraction

The time dependence of the gel fraction is compared for the PES polymers in Figure 3. Gelation occurred very quickly for both polymers, as a gel fraction of 0.22 was observed for PES<sub>b</sub> after only 5 min of reaction time. The increase in the gel fraction was less rapid for PES<sub>n</sub> where a gel fraction of 0.23 was formed after 30 min. A short induction period was apparent for PES<sub>n</sub> as the sharp rise occurred after 25 min. The gel fraction appeared to level off at a value of approximately 0.60 for PES<sub>b</sub> and approximately 0.75 for PES<sub>n</sub> after increasing monotonically. The steep rise in the

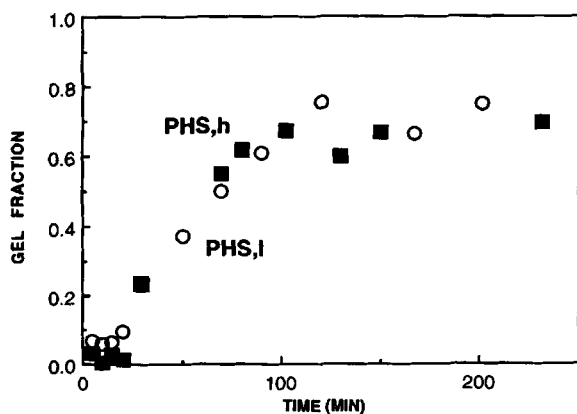


**Figure 4** Comparison of the temporal variations of gel formation for PHS polymers with different initial molecular weight values (PHS<sub>h</sub> = high; PHS<sub>l</sub> = low).

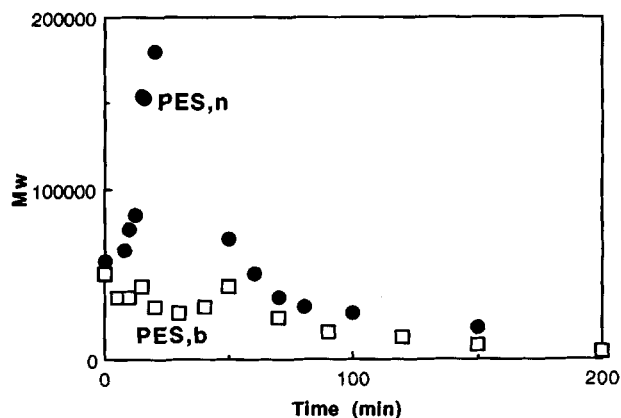


**Figure 5** Comparison of the temporal variations of weight average molecular weight ( $M_w$ ) changes for PES polymers with different initial molecular weight distributions (PES<sub>b</sub> = broad; PES<sub>n</sub> = narrow).

gel fraction from 0 to 20 min is akin to the critical gelation point of polymerization.

Comparison of the formation of a gel fraction for the PHS polymers is shown in Figure 4. The general shape of the time history is similar to that observed for PES. However, the critical gelation point, where the sharp rise begins, is shifted to longer reaction times. After 50 min, the gel fraction was 0.38 for PHS<sub>l</sub> and 0.44 for PHS<sub>h</sub>. Careful inspection of the two PHS curves reveals the gel fraction formed was slightly higher for reaction times up to 100 min for the PHS polymer with the higher initial weight average molecular weight.

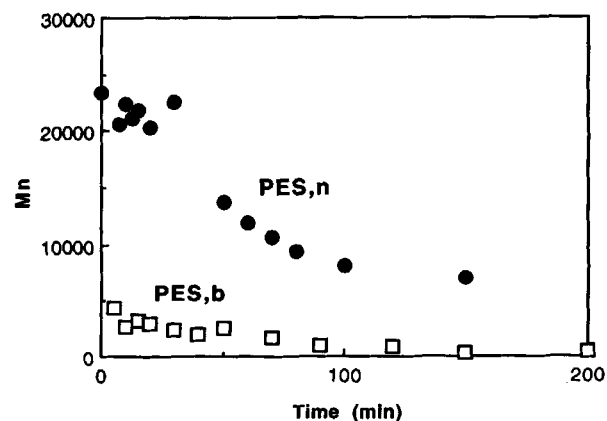


**Figure 6** Comparison of the temporal variations of number average molecular weight ( $M_n$ ) changes for PES polymers with different initial molecular weight distributions (PES<sub>b</sub> = broad; PES<sub>n</sub> = narrow).

### Sol Fraction Molecular Weight Distribution

The weight average molecular weight,  $M_w$ , and the number average molecular weight,  $M_n$ , are compared for PES polymers in Figures 5 and 6. The sol fraction  $M_w$  of  $PES_n$  initially increased sharply then monotonically decreased. The increase occurred at times below the critical gelation point. As the molecular weight continued to increase, a fraction was formed which was large enough to be filtered off. This defined the gel fraction. The  $M_w$  of the sol fraction correspondingly dropped at this point.

Similar behavior was not observed for the  $M_w$  changes of  $PES_b$ . The appearance of the gel fraction for  $PES_b$  as early as 2.5 min accounts for this difference. The kinetics leading to molecular weight increase, and thus gel formation, were too rapid to be captured on the time scale of the sol fraction  $M_w$  measurement. The weight average molecular weight rose rapidly in the first 5 min. Thus, the  $M_w$  results reported reflect only the period of monotonic decrease after a significant gel fraction was filtered off.

In contrast with  $M_w$ , the number average molecular weight decreased monotonically for both PES polymers. The simultaneous increase in  $M_w$  and decrease in  $M_n$  observed provide early evidence for the occurrence of two different types of controlling reactions. Bond breaking, or chain scission, reactions result in a decrease in polymer chain length. Bond forming, or addition, reactions lead to an increase in polymer chain length.

The similar time variations of  $M_w$  and  $M_n$  observed for the PHS polymers are shown in Figures 7 and 8.  $PHS_h$  showed a faster initial increase in  $M_w$  than  $PHS_l$ . This was followed by a sharp drop at a

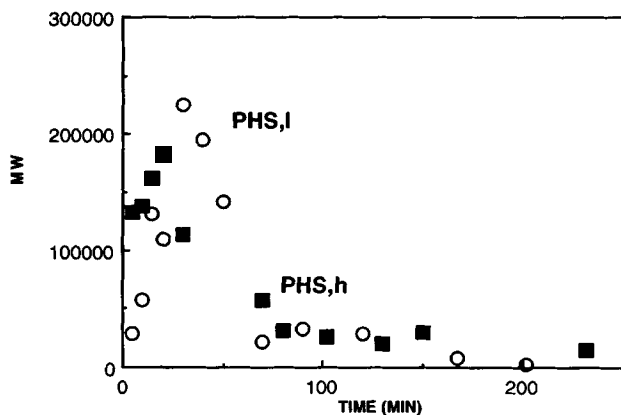


**Figure 7** Comparison of the temporal variations of weight average molecular weight ( $M_w$ ) for PHS polymers with different initial molecular weight values ( $PHS_h$  = high;  $PHS_l$  = low).

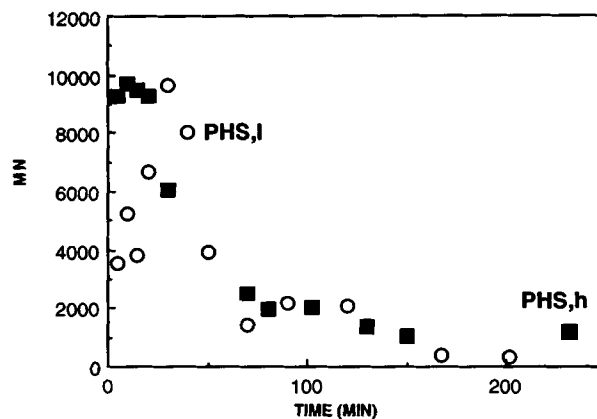


**Figure 8** Comparison of the temporal variations of number average molecular weight ( $M_n$ ) for PHS polymers with different initial molecular weight values ( $PHS_h$  = high;  $PHS_l$  = low).

shorter reaction time for  $PHS_h$  before both polymers underwent monotonic decrease in  $M_w$  at longer reaction times.  $PHS_h$  exhibited the same monotonic decrease in  $M_n$  observed for the PES polymers. In contrast,  $M_n$  for  $PHS_l$  increased slightly before monotonically decreasing after 40 min. Note the low  $M_n$  values achieved at long reaction times for both polymers. The sol fraction at this point consisted of a large fraction of short polymer chains.

Overall, clear trends were observed when the experimental results for PES and PHS polymer pairs were compared. The gel fraction and  $M_w$  values increased faster for  $PES_b$  and  $PHS_h$  than for  $PES_n$  and  $PHS_l$ , respectively. All polymers except  $PHS_l$  showed a sharp rise in  $M_w$  with a concomitant, steady decrease in  $M_n$ .

### RESULTS ANALYSIS: SIMULATION OF MOLECULAR WEIGHT CHANGES

The experimental results present indirect evidence of the underlying fundamental chemistry. The measured quantities are global in nature but a direct consequence of reactions occurring in the melt. The evolution of  $SO_2$  and the decrease in  $M_n$  and eventual decrease in  $M_w$  after long reaction times suggest the occurrence of bond scission reactions. The initial rapid rise in  $M_w$  and the formation of a gel fraction suggest the occurrence of bond forming, or addition, reactions. Quantitative resolution of the roles of bond forming and bond breaking, crucial to the eventual manipulation of these phenomena, is confronted with the statistical complexity of possible

events. This suggested a useful role for computer modeling as an accounting tool.

To this end, a Monte Carlo kinetics simulation was developed to probe the dependence of the observed experimental changes on the initial molecular weight distribution and the relative contributions of bond scission and bond formation. Input to the simulation consisted of the chain length distribution representative of a poly(arylether sulfone). The probability for bond scission,  $R$ , was varied as a parameter of the simulation.  $R$  was explicitly defined as

$$R = \frac{r_{\text{scission}}}{r_{\text{scission}} + r_{\text{addition}}}$$

A discrete number of reactions was carried out, and the resultant changes in  $M_w$  and  $M_n$  were recorded. Results for polymers with different initial molecular weight distributions parametric in the bond scission probability are considered here.

### Representation of Initial Polymer

The chain length distribution representing the initial polymer is a direct consequence of the molecular weight distribution of interest. Two different types of distributions were used to approximate the polymers studied experimentally: broad and monodisperse. One broad distribution with a polydispersity of 3.67 and an  $M_w$  of 65,000 and a second with a polydispersity of 2.72 and an  $M_w$  of 25,000 were derived from two representative PHS experimental distributions determined by gel permeation chromatography. Monodisperse distributions as limiting cases of narrow distributions were constructed for  $M_w = 65,000$  and  $M_w = 25,000$ . The choice of these four distributions allowed study of the effect of both initial weight average molecular weight and the breadth of the initial distribution on the observed  $M_w$  and  $M_n$  changes.

Determination of the total number of polymer chains in the simulation sample was guided by the initial molecular weight distribution. A typical pyrolysis reaction sample of 0.040 g with  $M_{w_0} = 25,000$  is composed of  $O(10^{18})$  polymer chains. Clearly, explicit treatment of this number of chains in the simulation is prohibitive. For simplicity, the number of chains in the simulation sample was calculated by extracting the minimal representative volume fraction of the melt that contained a single chain of the longest length in the distribution. The number of chains of other lengths was calculated from their

relative weight fractions of the distribution using the relationship shown as Eq. (1).

$$N_i = \frac{w_i}{w_{\text{max } j}} \frac{M_{\text{max } j}}{M_i} \quad (1)$$

In eq. (1),  $N_i$  is used to denote the number of chains of length  $i$ ,  $w_i$  is the weight fraction of chains of length  $i$ , and  $M_i$  is the molecular weight of a chain of length  $i$ . The molecular weight distribution of the overall sample is equivalent to the distribution of this representative sample.

### Reaction of the Polymer

Implementation of the scission and addition reactions was carried out stepwise. The type of reaction occurring during the current iteration was determined first. This was accomplished by comparing a drawn random number to the relative rate ( $0 \leq R \leq 1$ ) of bond scission to overall reaction. This measure of the overall global kinetics was supplied as an input parameter to the simulation.

Execution of a scission reaction first requires selection of one chain in the polymer melt. The chain that undergoes scission is chosen according to the probability a chain of a given length has of breaking. The appropriate measure is the number of chains with a given chain length weighted according to their chain length. This weighting reflects the chemistry of bond fission. When the points of chain scission in the poly(arylether sulfone) systems are the sulfone and ether linkages, a longer chain with more backbone linkages has a higher probability of undergoing scission. The length fraction,  $f_i$ , for a single chain of length  $i$ , is calculated as the length of the given chain in monomer units divided by the total number of monomers. This is represented by eq. (2):

$$f_i = \frac{i}{\sum_j (N_j j)} \quad (2)$$

A drawn random number determines the chain  $k$  that undergoes scission, according to eq. (3):

$$F_{k-1} < r_i < F_k \quad (3)$$

where  $F$  denotes the cumulative length fraction.

The point along the chain at which chain  $k$  undergoes scission is determined by drawing a second random number,  $r_j$ . The length of the first newly formed chain is calculated by multiplying  $r_j$  ( $0 < r_j < 1$ ) by the length of chain  $k$ . The length of the

second chain is simply obtained by difference. The total number of chains in the melt is increased by 1. Net bond scission is effected by simply capping the chains at their current length. This is chemically realized in the poly(arylether sulfone) systems through abstraction of hydrogen by a scission-derived phenyl radical or termination via recombination or disproportionation with  $H\cdot$ .

Net bond formation requires two chains, one of which "adds" to the other to realize net formation of a bond. The chains for addition are chosen by comparing two new random numbers,  $r_l$  and  $r_m$ , to the array of length fractions and choosing the chains that satisfies the criteria of eqs. (4) and (5):

$$F_{i-1} < r_l < F_i \quad (4)$$

$$F_{j-1} < r_m < F_j \quad (5)$$

This array contains the same weighted length fractions used to identify the initial scission chain. This use of the weighted fractions is guided by the chemistry proposed to account for bond formation, or crosslinking, in the poly(arylether sulfone) polymers.<sup>3-7,9,11</sup> Scission-derived phenyl radicals can add to the benzene rings of another polymer chain to form a cyclohexadienyl radical. Subsequent H-elimination regains the aromaticity, and a net crosslink links the two chains. Thus, the longer a given chain, the more possible points of addition it possesses. The length of the new chain is the sum of the lengths of the two individual chains. The total number of chains in the melt is decremented by 1.

The number average and weight average molecular weights are calculated for the new distribution

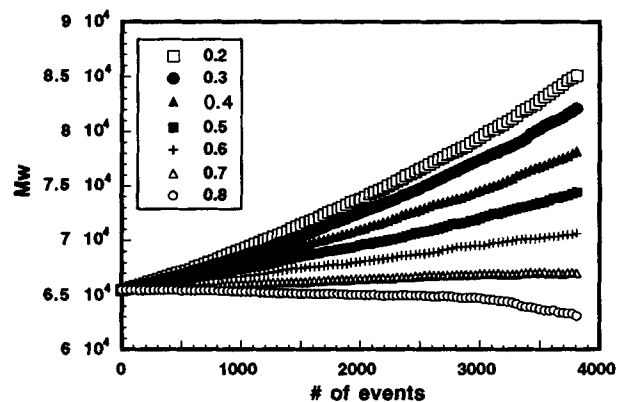


**Figure 9** Simulated changes in  $M_w$  as a function of the number of reaction events for a broad distribution with  $M_{w_0} = 65,000$ . Changes are reported parametric in  $R$ , the probability for bond scission.

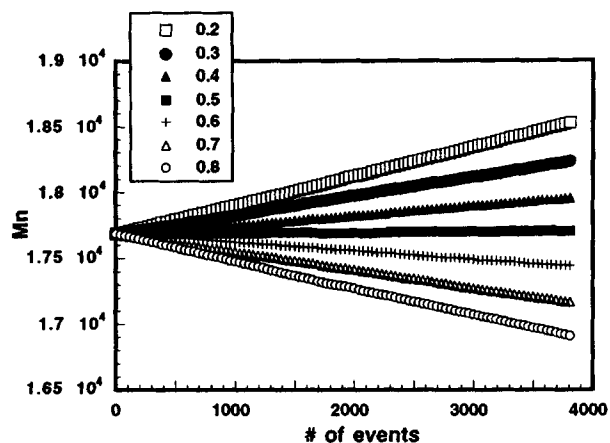


**Figure 10** Simulated changes in  $M_n$  as a function of the number of reaction events for a broad distribution with  $M_{w_0} = 65,000$ . Changes are reported parametric in  $R$ , the probability for bond scission.

of chain lengths and the updated total number of chains after the particular reaction has occurred. The new length fractions are calculated and the next reaction event is carried out. The simulation halts when a prespecified number of reaction events has taken place.

## SIMULATION RESULTS

The simulation results provided insight into the dependence of the observed experimental changes in  $M_w$  and  $M_n$  on the relative rates of bond scission and bond formation, the initial value of  $M_w$  and the breadth of the molecular weight distribution. To recapitulate, the increase in  $M_w$  and the concomitant decrease in  $M_n$  suggested the simultaneous occurrence of scission and addition reactions. Overall, the time scale for gelation and molecular weight changes decreased as the initial molecular weight distribution of a polymer with a given monomeric unit was broadened or the initial weight average molecular weight was increased.

### Ratio of Controlling Reactions

The simulations showed that only a certain range of bond scission probabilities was capable of reproducing the trends in  $M_w$  and  $M_n$  observed experimentally. The range of possible  $R$  values was dependent upon the breadth of the initial distribution. The evolution of  $M_w$  and  $M_n$ , parametric in  $R$ , is

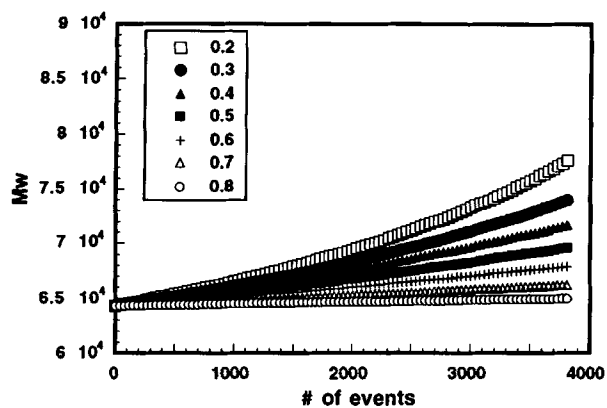


**Figure 11** Simulated changes in  $M_w$  as a function of the number of reaction events for a monodisperse distribution with  $M_{w_0} = 65,000$ . Changes are reported parametric in  $R$ , the probability for bond scission.

plotted in Figures 9 and 10 for the broad distribution with  $M_{w_0} = 65,000$  and in Figures 11 and 12 for the monodisperse distribution with  $M_{w_0} = 65,000$ . For both distributions,  $M_n$  decreased monotonically when  $R$  was greater than 0.5. However,  $M_w$  of the broad distribution, with its significant fraction of short chains in the low-molecular-weight tail of the initial melt, decreased below  $M_{w_0}$  for  $R = 0.8$  and was relatively flat for  $R = 0.7$ . These results suggest that there is a relatively fine balance between scission and addition that results in an increase in  $M_w$  and a simultaneous decrease in  $M_n$ . The range of the parameter  $R$  that is relevant to the PAES polymers studied is  $0.5 < R < 0.8$ .

The results of the simulation agree well with the results obtained by Kuroda et al.<sup>9</sup> They examined the dependence of the changes in  $M_w$  and  $M_n$  on the ratio of scission to crosslinking for a single initial distribution. The ratio of the number of scissions to the number of crosslinks,  $p$ , was varied. The ratio  $p$  is related to  $R$  of this simulation by eq. (6).

$$R = \frac{p}{p + 1} \quad (6)$$

$M_n$  was unchanged for  $p = 1$ , which is equivalent to  $R = 0.5$ .  $M_w$  increased with a simultaneous decrease in  $M_n$  for  $1 < p < 4$ , which translates to  $R$  falling in the range 0.5–0.8. However, the dependence of these limits on the initial molecular weight distribution was not reported.

### Breadth of the Distribution

Further examination of Figures 9–12 reveals sensitivity in the magnitude of the change in  $M_w$  and

$M_n$  to the breadth of the distribution. For values of  $R < 0.7$ , the rate of increase of  $M_w$  was greater for the broad distribution. For example, the highest molecular weight achieved for the broad distribution for  $R = 0.2$  was 85,000, whereas  $M_w$  for the monodisperse distribution was 78,000 for the same  $R$ . The selective addition to longer chains in the high molecular weight tail of the broad distribution accounts for these differences.

These results are consistent with experimental observations. PES<sub>b</sub> showed a faster increase in  $M_w$  and more rapid formation of a gel fraction than did PES<sub>n</sub>. The molecular weight achieved in the simulation after the prespecified  $1 \times 10^4$  reaction events was not high enough to be considered part of a gel fraction. However, extrapolation of the current slopes provides a qualitative estimation of gel formation and is consistent with the trends observed experimentally.

### Magnitude of $M_{w_0}$ and $M_{n_0}$

The dependence of the molecular weight changes on the values of  $M_{w_0}$  and  $M_{n_0}$  was assessed by comparing the simulation results reported above to those obtained for  $M_{w_0} = 25,000$ . The broad distribution results for  $M_w$  and  $M_n$  are reported in Figures 13 and 14, and the monodisperse results are plotted in Figures 15 and 16, parametric in  $R$ . In general, the greater the value of  $M_{w_0}$ , the larger the absolute change in  $M_w$  for a particular value of  $R$  and a given number of reaction events. This is consistent with the experimental results reported for PHS, where the higher initial molecular weight led to more rapid increases in  $M_w$  and faster gelation.

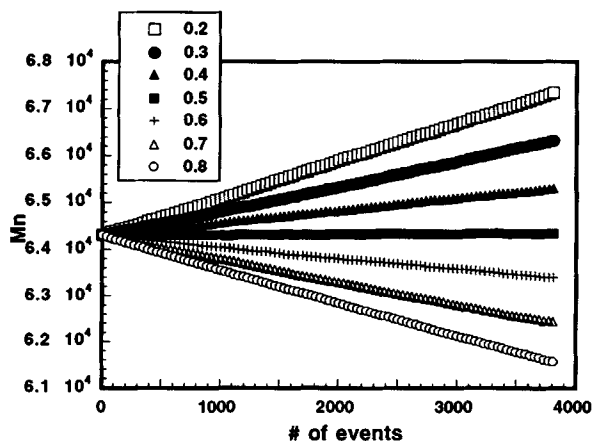


**Figure 12** Simulated changes in  $M_n$  as a function of the number of reaction events for a monodisperse distribution with  $M_{w_0} = 65,000$ . Changes are reported parametric in  $R$ , the probability for bond scission.



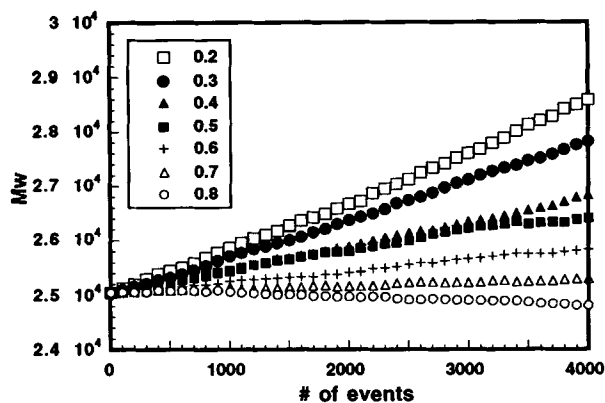


**Figure 13** Simulated changes in  $M_w$  as a function of the number of reaction events for a broad distribution with  $M_{w_0} = 25,000$ . Changes are reported parametric in  $R$ , the probability for bond scission.

The change in  $M_n$  was linear for all initial distributions. Normalization of the slopes by  $M_{n_0}$  resulted in values differing by less than  $1.2 \times 10^{-7}$  for  $R = 0.8$ . The steepest absolute decline was observed for the largest value of  $M_{n_0} = 65,000$ . This reproduces the PES experimental data well, where the initial decrease in  $M_n$  was fastest for PES<sub>n</sub>. The absolute change in  $M_n$  is more relevant than the normalized one, since the rapid appearance of a significant fraction of short chains can result in a significant deviation in polymer properties from those initially designed.

## CONCLUSIONS

Reaction of poly(arylether sulfones) under thermally severe conditions resulted in the formation of an in-

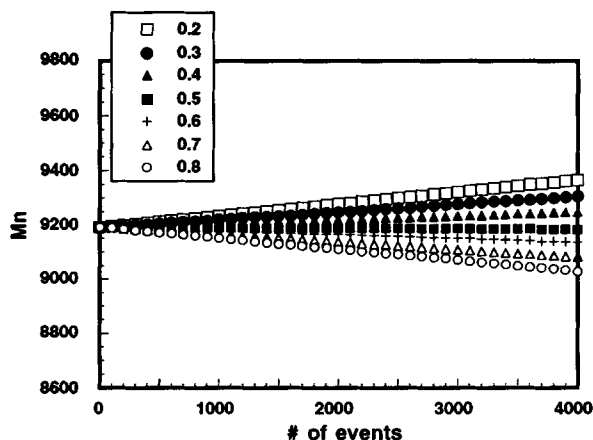


**Figure 14** Simulated changes in  $M_n$  as a function of the number of reaction events for a broad distribution with  $M_{w_0} = 25,000$ . Changes are reported parametric in  $R$ , the probability for bond scission.

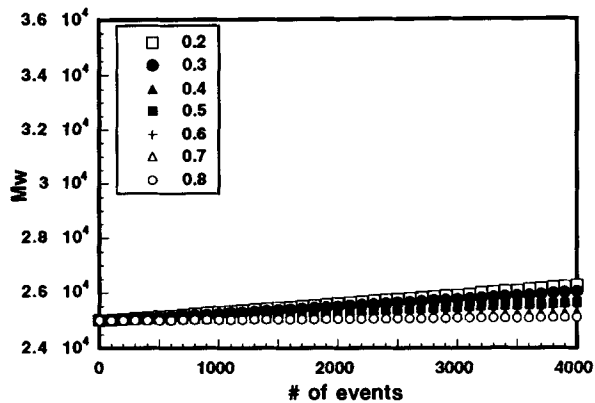


**Figure 15** Simulated changes in  $M_w$  as a function of the number of reaction events for a monodisperse distribution with  $M_{w_0} = 25,000$ . Changes are reported parametric in  $R$ , the probability for bond scission.

soluble gel fraction and significant changes in weight average and number average molecular weight of the sol fraction. The magnitude of the changes observed was dependent upon the chemical composition of the polymer backbone and the physical attributes of the polymer. The PAES with an alternating sequence of ether and sulfone linkages formed a larger fraction of gel at a given reaction time than the PAES with the hydroquinone moiety. For a given chemical composition, more rapid molecular weight changes and gel fraction formation were observed for the polymer with the higher value of weight average molecular weight. Similarly, molecular weight growth was faster for the polymer with the broader initial distribution.

The simultaneous increase in  $M_w$  and decrease in  $M_n$  suggested the occurrence of two types of overall

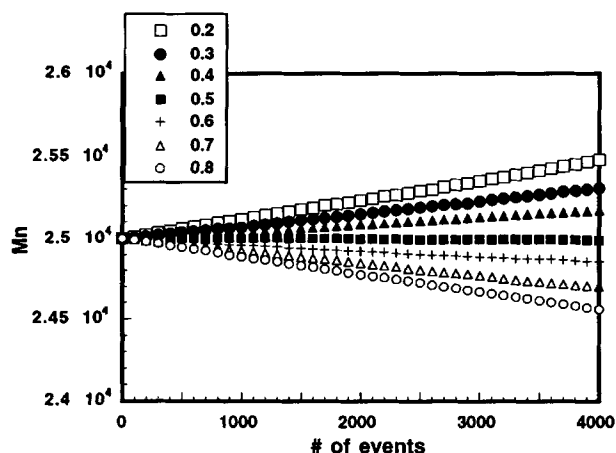


**Figure 16** Simulated changes in  $M_n$  as a function of the number of reaction events for a monodisperse distribution with  $M_{w_0} = 25,000$ . Changes are reported parametric in  $R$ , the probability for bond scission.

reactions: scission and addition. Simulation of these two types of reactions using Monte Carlo kinetics allowed estimation of the ratio of the reaction rates capable of accounting for the observed experimental behavior. The ratio of the rate of scission to the overall rate of reaction was greater than 0.5 to achieve a decrease in  $M_n$ . The dependence of the simulated molecular weight changes on the initial molecular weight distribution was in qualitative agreement with the experimental trends.

## REFERENCES

1. K. V. Gotham and S. Turner, *Polymer*, **15**, 665 (1974).
2. J. B. Rose, *Polymer*, **15**, 456 (1974).
3. W. F. Hale, A. G. Farnham, R. N. Johnson, and R. A. Clendinning, *J. Polym. Sci., Part A-1*, **5**, 2399 (1967).
4. I. I. Levantovskaya, G. V. Dralyuk, O. A. Mochalova, I. A. Yurkova, M. S. Akutin, and B. M. Kovarskaya, *Vysok. Soyed.*, **1**, 8 (1971).
5. B. Crossland, G. J. Knight, and W. W. Wright, *Br. Polym. J.*, **18**(3), 156 (1986).
6. L. I. Danilina, E. N. Teleshov, and A. N. Pravednikov, *Vysok. Soyed.*, **3**, 581 (1974).
7. A. Davis, *Makromol. Chem.*, **128**, 242 (1969).
8. A. Charlesby and S. H. Pinner, *Proc. Roy. Soc. London A*, **249**, 367 (1959).
9. S. Kuroda, K. Terauchi, K. Nogami, and I. Mita, *Eur. Polym. J.*, **25**(1), 1 (1989).
10. A. L. Nakron, I. I. Levantovskaya, V. V. Gur'yanova, L. I. Reitburd, O. V. Yershov, G. V. Dralyuk, M. A. Motorina, Ye. I. Metelkina, L. M. Bolotina, A. B. Blyumenfel'd, and A. V. Pavlov, *Polym. Sci. USSR*, **28**(3), 562 (1986).
11. C. Libanati, L. Broadbelt, C. LaMarca, M. T. Klein, S. M. Andrews, and R. J. Cotter, *Mol. Simulation*, **11**(2-4), 187 (1993).

Received August 29, 1994

Accepted May 18, 1995